Journal of Physics: Condensed Matter

PAPER

Angle-resolved photoemission spectroscopy observation of anomalous electronic states in $EuFe_2As_{2-x}P_x$

To cite this article: P Richard *et al* 2014 *J. Phys.: Condens. Matter* **26** 035702

IOP Publishing Journal of Physics: Condensed Matter

J. Phys.: Condens. Matter **26** (2014) 035702 (8pp) doi:10.1088/0953-8984/26/3/035702

Angle-resolved photoemission spectroscopy observation of anomalous electronic states in $EuFe_2As_{2-x}P_x$

P Richard[1,2], C Capan[3,4], J Ma[1], P Zhang[1], N Xu[1,5], T Qian[1], J D Denlinger[6], G-F Chen[1], A S Sefat[7], Z Fisk[3] and H Ding[1,2]

[1] Beijing National Laboratory for Condensed Matter Physics, and Institute of Physics, Chinese Academy of Sciences, Beijing 100190, People's Republic of China
[2] Collaborative Innovation Center of Quantum Matter, Beijing, People's Republic of China
[3] Department of Physics and Astronomy, University of California, Irvine, CA 92697, USA
[4] Department of Physics, Washington State University, Pullman, WA, USA
[5] Paul Scherrer Institut, Swiss Light Source, CH-5232 Villigen PSI, Switzerland
[6] Advanced Light Source, Lawrence Berkeley National Laboratory, Berkeley, CA 94720, USA
[7] Materials Science and Technology Division, Oak Ridge National Laboratory, Oak Ridge, TN 37831-6114, USA

E-mail: p.richard@iphy.ac.cn

Received 28 October 2013, revised 20 November 2013
Accepted for publication 20 November 2013
Published 18 December 2013

Abstract

We used angle-resolved photoemission spectroscopy to investigate the electronic structure and the Fermi surface of $EuFe_2As_2$, $EuFe_2As_{1.4}P_{0.6}$ and $EuFe_2P_2$. We observed doubled core level peaks associated with the pnictide atoms. Using K atoms evaporated at the surface to affect the surface quality, we show that one component of these doubled peaks is related to a surface state. Nevertheless, strong electronic dispersion along the *c*-axis, especially pronounced in $EuFe_2P_2$, is observed for at least one band, thus indicating that the Fe states, albeit probably affected at the surface, do not form pure two-dimensional surface states. We determine the evolution of the Fermi surface as a function of the P content and reveal that the hole Fermi surface pockets enlarge with increasing P content. We also show that the spectral weight near the Fermi level of $EuFe_2P_2$ is reduced as compared to that of $EuFe_2As_2$ and $EuFe_2As_{1.4}P_{0.6}$. Finally, we identify the electronic states associated with the Eu^{2+} f states and show an anomalous jump in $EuFe_2P_2$.

Keywords: Fe-based superconductors, ARPES, $EuFe_2P_2$, electronic structure

(Some figures may appear in colour only in the online journal)

1. Introduction

Although not as extensively studied as the $Ba_{1-x}K_xFe_2As_2$ and $BaFe_{2-x}Co_xAs_2$ archetype systems of 122-ferropnictides, the $EuFe_2As_{2-x}P_x$ compounds show very unique and exotic properties, which vary significantly upon As → P isovalent substitution. In addition to a magnetic Fe network, a large moment is observed on the Eu^{2+} ions [1–5]. While the Eu sublattice exhibits A-type antiferromagnetism below T_N = 19 K in $EuFe_2As_2$ [3, 6], a ferromagnetic structure with slightly canted Eu moments aligned along the *c*-axis is observed in $EuFe_2P_2$ below T_N = 30 K [4, 5]. The Eu atoms also seem to play an essential role in the anomalous compressibility effects observed in $EuFe_2As_2$ [7], and a Eu valence change under pressure has even been reported in superconducting $EuFe_2As_{1.4}P_{0.6}$ [8].

Especially following the discovery of reentrant superconductivity in $EuFe_2As_{1.3}P_{0.7}$ coinciding with the ordering of the Eu^{2+} moments [2], the detail of the interplay between the Eu^{2+} and Fe^{2+} layers, as well as the precise role

of the As → P isovalent substitution for the emergence of superconductivity, became important issues that are still debated and need proper experimental characterizations. With its capacity to resolve the one-particle electronic spectra of materials directly in the momentum space, angle-resolved photoemission spectroscopy (ARPES) is a powerful tool that may be used for such purposes. Indeed, the electronic structures of the $EuFe_2As_2$ parent compound [9–11] and of $EuFe_2As_{1.56}P_{0.44}$ [11] have been studied by ARPES recently. Although it was first synthesized [12] three decades before the discovery of Fe-based superconductivity in 2008 [13], there is unfortunately no ARPES report in the literature on the electronic structure of $EuFe_2P_2$.

In this paper, we present an ARPES study of the electronic structure of $EuFe_2As_{2-x}P_x$, from $EuFe_2As_2$ to $EuFe_2P_2$. The photoemission spectra indicate that all these materials have at least two inequivalent pnictide sites, which is linked to a surface state possibly resulting from the pnictide–pnictide interactions occurring in short *c*-axis 122 compounds. Nevertheless, we record strong modulations of the electronic structure along the perpendicular momentum (k_z) direction, which become more prominent upon As → P substitution. We also observe an unexplained jump in the energy position of the Eu^{2+} f electrons in $EuFe_2P_2$.

2. Experiment

Single crystals of $EuFe_2As_2$, $EuFe_2As_{1.4}P_{0.6}$ and $EuFe_2P_2$ were grown using conventional methods described in [14, 8, 15]. While the typical size of the samples of the first two compounds exceeds 1.5 × 1.5 mm^2, much smaller samples (around 150 × 150 μm^2) of $EuFe_2P_2$ were measured. Most of the ARPES measurements were made at the PGM and APPLE-PGM beamlines of the Synchrotron Radiation Center (Wisconsin) equipped with a VG Scienta R4000 analyser and an SES 200 analyser, respectively. The energy and angular resolutions for the angle-resolved data were set at 10–30 meV and 0.2°, respectively. The samples were cleaved *in situ* and measured at 20 K in a vacuum better than 5 × 10^{-11} Torr. Additional core level measurements of the $EuFe_2As_2$ surface under potassium evaporation were made at the Merlin beamline of the Advanced Light Source (California). Throughout the paper, we label the momentum values with respect to the 1 Fe/unit-cell Brillouin zone (BZ), and use $c' = c/2$ as the distance between two Fe planes.

3. Results and discussion

In figure 1(a), we compare the core level spectra of $EuFe_2As_2$, $EuFe_2As_{1.4}P_{0.6}$ and $EuFe_2P_2$, which show signatures of the elemental composition of these materials. We first describe the features observed above 20 eV of binding energy (E_B). All spectra contain a very small peak detected around E_B = 91.3 eV that we assign to the Fe 3s electronic state, as well as a well defined and more intense peak associated with the Fe 3p electrons, which is observed at an E_B of 52.4 eV, 52.6 eV and 52.9 eV in these three compounds, respectively. As emphasized in the middle inset, a broad bump absent from $EuFe_2As_2$ but increasing with P substitution is also observed at a slightly higher E_B (60.7 eV). This bump is detected at the same kinetic energy of 115.3 eV, independently of the incident photon energy, and we thus attribute it to Auger electrons from P.

The most intense peaks observed in $EuFe_2As_2$ and $EuFe_2As_{1.4}P_{0.6}$ correspond to the As $3d_{3/2}$ and $3d_{5/2}$ states. A zoom, displayed in the right inset of figure 1(a), shows an average shift of 75 meV towards high E_B in $EuFe_2As_{1.4}P_{0.6}$ as compared to $EuFe_2As_2$. More importantly, we observe that these peaks are doubled, indicating the presence of two inequivalent As sites, suggesting a surface reconstruction affecting directly the As electronic states. When increasing the P content from $x = 0$ to $x = 0.6$, the splittings between the peaks associated with the two sites increase slightly, from 237 meV to 248 meV, and from 225 meV to 240 meV for the As $3d_{3/2}$ and As $3d_{5/2}$ states, respectively. As expected from their equivalent role in the structure of $EuFe_2As_{2-x}P_x$, double-peak features are also observed for the P $2p_{1/2}$ and P $2p_{1/2}$ electronic states in the P-substituted materials. As shown in the left inset of figure 1(a), the splitting between the two sites increases significantly as the P concentration is raised from $x = 0.6$ to 2. Indeed, we record a splitting that increases from 206 to 522 meV for the P $2p_{1/2}$ states, and a splitting that increases from 210 to 519 meV for the P $2p_{3/2}$ states. It is important to note that while such effect on the pnictide atoms could potentially have a sizeable impact on the Fe electronic states in $EuFe_2As_{2-x}P_x$, our previous measurements [16] on a wide doping range of hole-doped $Ba_{1-x}K_xFe_2As_2$ and electron-doped $BaFe_{2-x}Co_xAs_2$ did not evidence any of these doubled features.

To determine whether the doubled features observed in these materials are related to a surface state or to an impurity phase, we evaporated successively small numbers of K atoms *in situ* on the cleaved surface of a $EuFe_2As_2$ sample and investigated the As 3d core levels. Such a process can damage the surface by introducing disorder, notably on polar surfaces likely to interact with the K^+ ions, thus suppressing the electronic surface states. As illustrated in figure 1(b), the high-E_B components of the As $3d_{3/2}$ and As $3d_{5/2}$ core levels are barely affected by this process, suggesting that they are related to bulk states. In contrast, the low-E_B components are rapidly suppressed upon K evaporation, which is consistent with the destruction of a surface state. We also observe a slight shift towards high E_B attributed to a shift of the chemical potential at the surface due to the electron doping induced by the K dopant atoms. As discussed below, the states within 3 eV below the Fermi level (E_F) are also affected (see figure 1(c)), though in a more complicated way.

Although they cannot be assigned unambiguously, additional peaks in the spectra of the P-substituted samples are observed in the 127 ≤ E_B ≤ 133 eV range. While some of them may also come from the P 2p states, we should expect that others may be related to the Eu 4d energy levels. Indeed, as shown in the left inset of figure 1(a), P-free $EuFe_2As_2$ exhibits a rather rich spectrum in this region: a series of peaks spaced by an average interval of 920 meV is observed

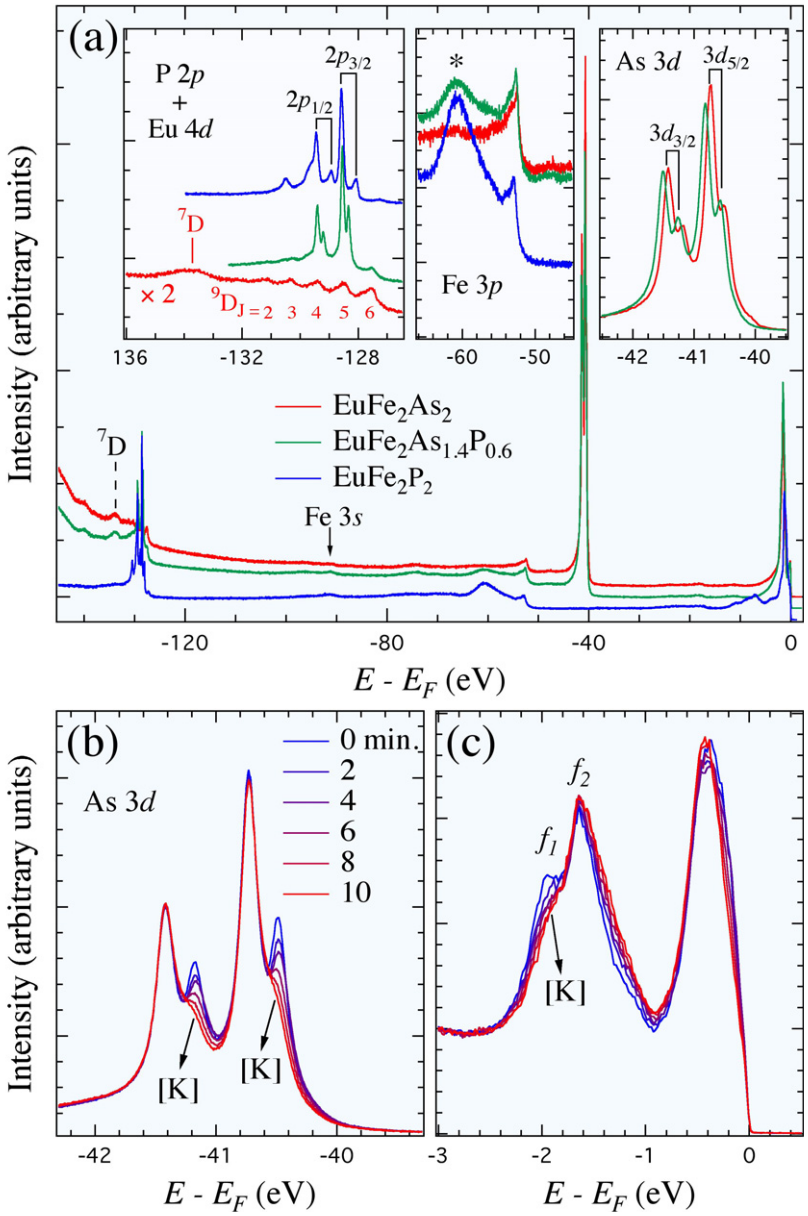

Figure 1. (a) Core level spectra of $EuFe_2As_{2-x}P_x$ recorded with 180 eV photons. The spectra have been shifted vertically for a better visualization. The left inset corresponds to the P 2p and Eu 4d spectral range, where the spectrum of $EuFe_2As_2$ has been multiplied by 2. Black lines are guides to the eye for the splitting between the peaks of two sites of P. The middle inset coincides with the Fe 3p spectral range. The asterisks refer to 115.3 eV Auger electrons from P. The right inset corresponds to the spectral range of As 3d electronic states. Black lines serve as guides to the eye for the separations between the peaks of two As sites. (b), (c) Evolution of the photoemission spectra as a function of the time of potassium evaporation, for the As 3d and the near-E_F spectral ranges, respectively.

at $E_B = 127.54$, 128.48, 129.40, 130.32 and 131.22 eV, in the proximity of a broader bump centred at $E_B = 133.8$ eV. Interestingly, similar features have been already reported in Eu metal [17] as well as in EuTe [18]. Starting from a Eu^{2+} ($4d^{10}4f^7$) initial state, the spectrum of Eu metal was interpreted in terms of the ^7D and ^9D spectroscopic terms of the Eu^{3+} ($4d^94f^7$) final state [17]. As in Eu metal, while the $^9D_{J=(2-6)}$ multiplets of the ^9D term can be identified in $EuFe_2As_2$, the ^7D term remains unresolved.

We now switch our attention to the electronic states forming the Fermi surface (FS) of $EuFe_2As_{2-x}P_x$. In figure 2, we compare the FSs of $EuFe_2As_2$, $EuFe_2As_{1.4}P_{0.6}$ and $EuFe_2P_2$, around $k_z = 0$ and π/c'. As with $BaFe_2As_2$, the FS of $EuFe_2As_2$ exhibits stronger spots of intensity, mainly visible around the M/A $[(0, \pi, k_z)]$ point, which are attributed to the presence of Dirac cones induced by the antiferromagnetic ordering [19]. As a result of a surface reconstruction similar to the one reported in $BaFe_{2-x}Co_xAs_2$ [20] and $Ca_{0.83}La_{0.17}Fe_2As_2$ [21], an extra pattern of intensity is observed at the X point.

As reported in a previous ARPES study of $EuFe_2As_{1.56}P_{0.44}$ [11] and commonly expected for an Fe-based superconductor with the 122 crystal structure and a non-magnetically ordered Fe network [22], the FS of

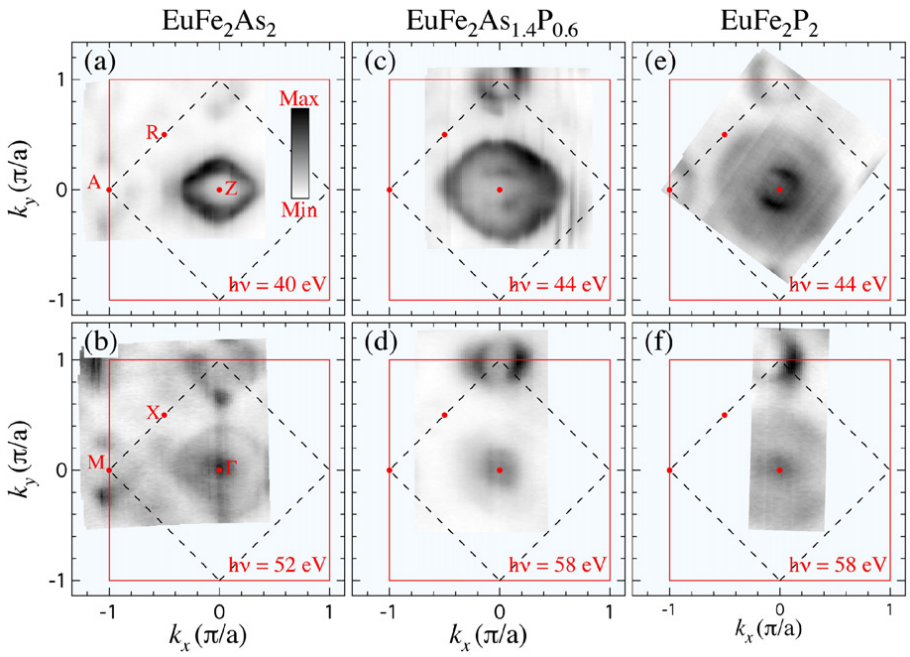

Figure 2. Fermi surface mappings of $EuFe_2As_2$ ((a) and (b)), $EuFe_2As_{1.4}P_{0.6}$ ((c) and (d)) and $EuFe_2As_2$ ((e) and (f)), obtained by integrating the photoemission intensity within ±5 meV of E_F. The top and bottom rows refer to mappings recorded with $k_z \sim \pi/c'$ (Z) and $k_z \sim 0$ (Γ), respectively. The red squares define the in-plane projection of the 1 Fe/unit-cell BZ.

$EuFe_2As_{1.4}P_{0.6}$ and $EuFe_2P_2$ are composed by Γ-centred hole FS pockets and M-centred electron FS pockets. Their size evolves with the P content, but in a non-symmetrical way. While the FS pattern at the M point becomes only a little smaller with x increasing from 0 to 2, the size of the Γ-centred pockets increases significantly, suggesting a hole doping that cannot be explained by a simple chemical potential shift, as also pointed out in a previous ARPES study [11]. According to our core level data reported above, we cannot exclude the possibility that this non-trivial doping dependence might be related to a surface doping effect. However, the present case is quite different from the situations encountered for $YBa_2Cu_3O_{7-x}$ [23, 24] and the 1111-ferropnictides [25, 26]. In particular, the photoemission intensity mappings displayed in figure 2 for different photon energies indicate non-negligible electronic dispersion along k_z, thus suggesting that the low-energy states probed by ARPES cannot be pure two-dimensional surface states.

A better visualization of the electronic dispersion along k_z is provided by the photon energy dependence of the photoemission intensity along the Γ–M high-symmetry line of the three compounds measured in our study, which are shown in the top row of figure 3, as well as the curvature intensity plots [27] given in the bottom row of figure 3. Within the free-electron approximation, there is indeed a monotonic relationship between the incident photon energy and the perpendicular momentum k_z of the photoemitted electrons [28] that allows us to interpret these plots as FS mappings in the k_x–k_z plane. One of the bands, centred at $k_z = \pi/c'$, exhibits strong dispersion along k_z. In fact, the ARPES intensity plots displayed in figure 4 indicate that, while that band has a very large Fermi wavevector (k_F) around $k_z = \pi/c'$ (top panels of figure 4), it does not even cross E_F around $k_z = 0$ (bottom panels of figure 4) for any of the $EuFe_2As_{2-x}P_x$ materials studied here. In other words, this band forms a 3D hole pocket centred at Z, which becomes larger with increasing P content, an observation consistent with the large 3D FS suggested from de Haas–van Alphen measurements in $CaFe_2P_2$ [29], although that FS is even larger in the latter case. Interestingly, this band varies similarly to the α band in $Ba(Fe_{1-x}Ru_x)_2As_2$ [30–32], which is another nominally non-doped 122-ferropnictide. We thus assign to this band the same d_{even} main orbital character, d_{even} being the even combination of the d_{xz} and d_{yz} orbitals. Our photon energy dependence also indicates that the distance in photon energy between two successive Z points increases, which is consistent with the decrease in the c'-axis parameter when As atoms are substituted by smaller P atoms.

The spectral features shown in figure 3 are not as well defined in $EuFe_2P_2$ as in the samples with lower P content, an observation further evidenced by the ARPES intensity plots displayed in figure 4. In particular, the near-E_F spectral intensity around the Γ point of $EuFe_2P_2$ is quite weak (see figure 4(f)). This contrasts with the intensity of the ω band found at higher binding energy, which remains high for all x concentrations. In figure 5, we compare the photon energy dependence of the BZ centre energy distribution curves (EDCs) of $EuFe_2As_2$, $EuFe_2As_{1.4}P_{0.6}$ and $EuFe_2P_2$. The lower energy part of the EDCs is dominated by two peaks coming from the ζ and ω bands, which both have a dominant d_{z^2} character [33]. Neglecting small k_z and sample composition variations, these peaks are located around 170 and 530 meV below E_F, respectively. Interestingly, their intensity oscillates with photon energy (or k_z) in anti-phase,

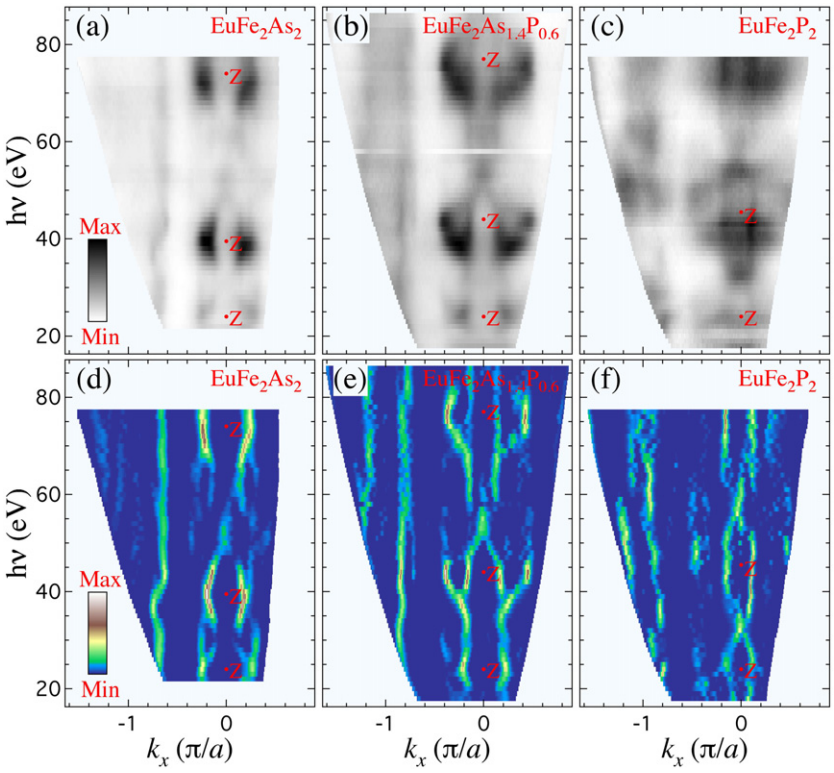

Figure 3. Photon energy dependence of the photoemission intensity at E_F (±5 meV integration) along Γ–M for (a) $EuFe_2As_2$, (b) $EuFe_2As_{1.4}P_{0.6}$ and (c) $EuFe_2P_2$, and (d)–(f) their corresponding intensity plots of 1D curvature (along k_x) [27].

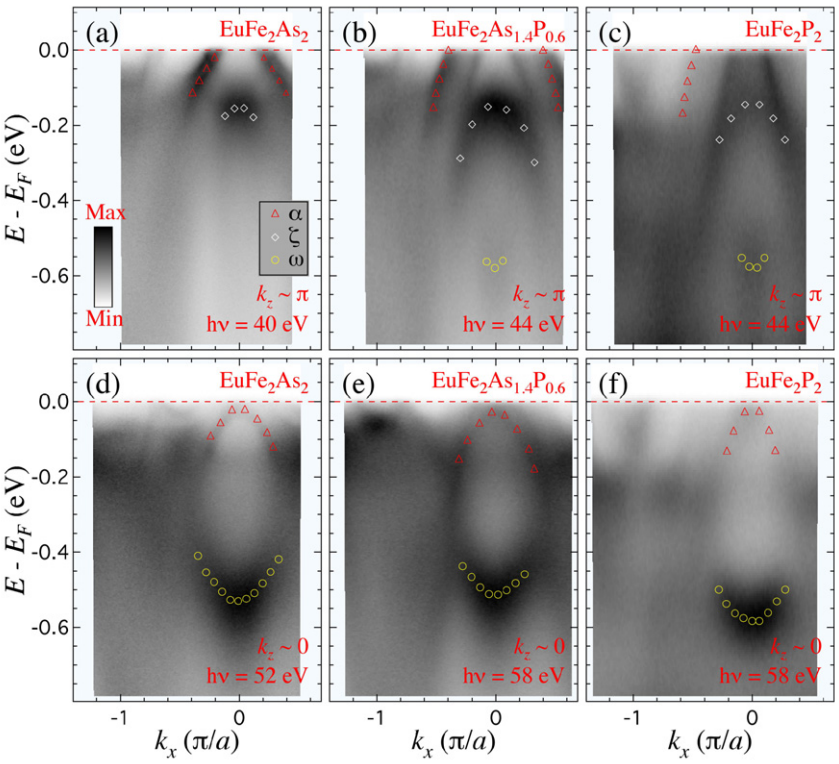

Figure 4. Top row: ARPES intensity plots along the Γ–M direction for $k_z \sim \pi$. Bottom row: same but for $k_z \sim 0$. The open symbols are guides to the eye for the α band with d_{even} orbital character, as well as for the ζ and ω bands, which both have a strong d_{z^2} component [33]. (a), (d) $EuFe_2As_2$, (b), (e) $EuFe_2As_{1.4}P_{0.6}$ and (c), (f) $EuFe_2P_2$.

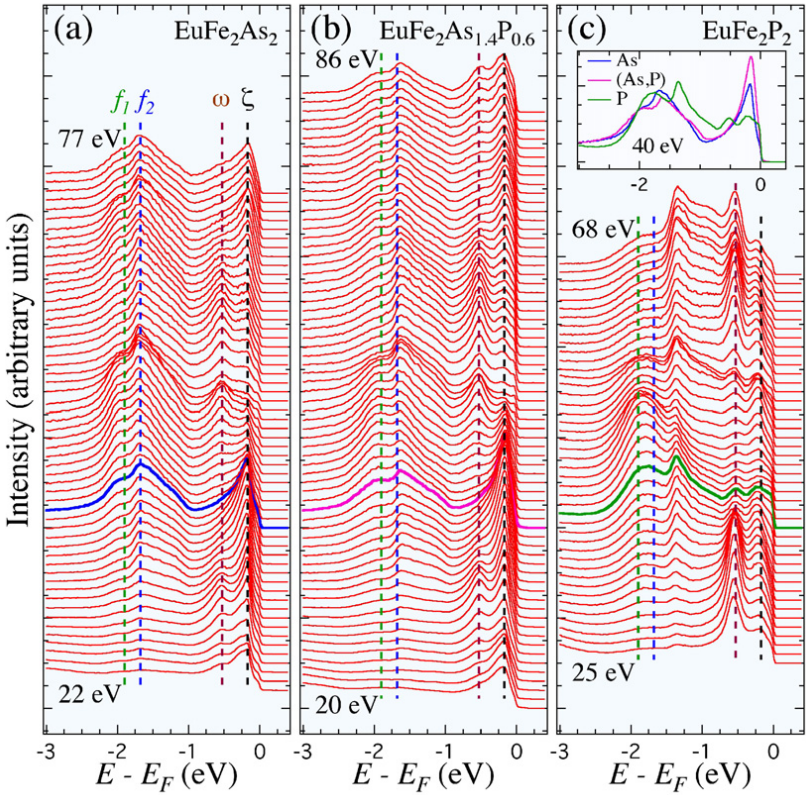

Figure 5. Photon energy dependence of the EDCs recorded at the BZ centre in (a) $EuFe_2As_2$, (b) $EuFe_2As_{1.4}P_{0.6}$ and (c) $EuFe_2P_2$. The inset in (c) compares the EDCs of the three compounds recorded with 40 eV photons. As, (As, P) and P refer to $EuFe_2As_2$, $EuFe_2As_{1.4}P_{0.6}$ and $EuFe_2P_2$, respectively. In each panel, the vertical lines are guides to the eye for the energy position of four peaks detected in $EuFe_2As_2$: f_1 (−1.9 eV), f_2 (−1.7 eV), ω (−0.53 eV) and ζ (−0.17 eV).

as also illustrated in figure 4. While the intensity of the ζ peak is the strongest around $k_z = \pi/c'$ and the weakest around $k_z = 0$, the opposite behaviour is found for the ω band. Although our study does not allow us to identify unambiguously the origin of the partial suppression of spectral intensity for the electronic states at low energy, it is possibly related to the surface state identified from the core level data presented in figure 1, which show significantly larger core level splittings in $EuFe_2P_2$. Distortion at the surface could eventually introduce additional scattering that would suppress the coherence of the low-energy states. We caution though that an old study of structural characterization revealed the presence of FeP or Fe_2P as secondary phase in the growth of some $LnFe_2P_2$ (Ln = lanthanide) compounds [34], which could also alter the coherence of the low-energy states. However, we did not detect evidence for these impurities in our samples.

In addition to the ζ and ω peaks, additional spectral intensity is found between 1 and 2.5 eV below E_F. In particular, a peak labelled f_2 and a shoulder labelled f_1 are detected in $EuFe_2As_2$ at −1.7 eV and −1.9 eV, respectively. These dispersionless features are not observed in the more commonly studied $Ba(Fe_{1-x}Co_x)_{2-x}As_2$ and $Ba_{1-x}K_xFe_2As_2$ compounds [16]. In agreement with a previous ARPES study [10], we ascribe them to Eu ^{4}f electronic states. As indicated by the inset of figure 5(c), which compares the EDCs of the three measured compounds recorded with 40 eV photons, only small changes occur when the P content varies from $x = 0$ to 0.6. While the f_1 peak position in $EuFe_2As_{1.4}P_{0.6}$ is barely changed, the f_2 peak moves by about 50 meV towards E_F. As illustrated in figure 5(c), the f_2 peak shift is much larger in $EuFe_2P_2$. As compared to $EuFe_2As_2$, the f_1 and f_2 peaks in $EuFe_2P_2$ are located 80 meV and 320 meV closer to E_F, respectively.

Such large splitting between the f_1 and f_2 peaks allows us to distinguish their spectral lineshapes, which are quite different. In contrast to the f_1 peak, which is quite broad and rounded, the f_2 peak is rather sharp. The latter is also asymmetric, with a tail on the low E_B side possibly due to the presence of additional peaks, as mainly suggested from the spectra recorded at the highest photon energies. Interestingly, as shown in figure 1(c), our investigation of the electronic states in a $EuFe_2As_2$ sample upon K evaporation on the surface indicates that, while the shape and intensity of the f_2 peak are barely modified by the evaporation of K atoms, the intensity of the f_1 peak is reduced, suggesting a surface state. However, this particular observation does not explain the large shift in the position of the f_2 peak in $EuFe_2P_2$. It is important to note that we did not observe any significant modification of the spectral lineshape across the Eu^{2+} magnetic ordering transition, thus suggesting that it is not relevant for this particular lineshape or for the large f_1–f_2 splitting in $EuFe_2P_2$. However, the inset of figure 5(c) seems to show that the shift of the f_2 peak in $EuFe_2P_2$ is accompanied by a spectral weight

transfer from the near-E_F states to the $0.5 \leq E_B \leq 1.5$ energy range. Whether this could be caused by enhanced Fe–Eu interactions is not excluded but would require confirmation from further theoretical investigations.

From the core levels to the electronic states in the vicinity of E_F, our results indicate the presence of a surface state effect in $EuFe_2As_{2-x}P_x$ that does not exist, or at least that does not manifest itself significantly, in the commonly studied $Ba(Fe_{1-x}Co_x)_{2-x}As_2$ and $Ba_{1-x}K_xFe_2As_2$ 122-ferropnictides. We note that the size of the Eu^{2+} ion is significantly smaller than that of Ba^{2+}, and the substitution of P by As contributes to reduce the c-axis length even further. Previous studies showed that, when the c-axis becomes small and the As–As separation in the 122-ferropnictides becomes smaller than about 3 Å, either due to rare earth substitution [35] or As → P substitution in $CaFe_2As_{2-x}P_x$ [36, 37], interactions between successive As layers induce a further decrease in the c-axis length of these materials that thus encounter a tetragonal-collapsed tetragonal transition [35], as also supported by theoretical predictions [38]. We point out that any material in the collapsed tetragonal phase or at the proximity of this transition may show a discontinuity in the pnictide–pnictide interactions at the surface, possibly altering the surface electronic properties. Indeed, a previous ARPES study revealed anomalies in conventional ARPES data recorded on $LaRu_2P_2$ as compared to bulk-sensitive soft-x-ray ARPES data [39]. We predict that other 122 materials with similarly small c-axis as $EuFe_2As_{2-x}P_x$ and $LaRu_2P_2$ may exhibit the same kind of anomaly reported here and in [39]. Yet, further theoretical and experimental investigations are necessary to confirm or reject this conjecture.

4. Summary

In summary, we performed an ARPES study of $EuFe_2As_{2-x}P_x$ that shows the evolution of the electronic structure upon increasing the P content. All the samples studied show an anomaly in the core levels of the pnictide atoms, which is strongly suppressed by evaporating K atoms on the surface, thus indicating the presence of a surface state. Nevertheless, strong k_z modulations enhanced with P substitution are observed in all samples for at least one band, revealing that the Fe electronic states do not form a pure surface state. Our comparison of the various FSs show that the size of the Γ-centred hole FS pockets increases with the P content. We also identified the Eu^{2+} f states at energies between 1 and 2.4 eV below E_F and found a sudden and unexplained jump in the energy position of one peak associated with the Eu^{2+} f states in $EuFe_2P_2$.

Acknowledgments

We acknowledge M Shi, E Razolli and J-X Yin for useful discussions. This work was supported by grants from CAS (2010Y1JB6), MOST (2010CB923000, 2011CBA001000, 2011CBA00102, 2012CB821403 and 2013CB921703) and NSFC (11004232, 11034011/A0402 and 11274362) from China. This work is based in part on research conducted at the Synchrotron Radiation Center, which is primarily funded by the University of Wisconsin–Madison with supplemental support from facility users and the University of Wisconsin–Milwaukee. The Advanced Light Source is supported by the Director, Office of Science, Office of Basic Energy Sciences, of the US Department of Energy under Contract No. DE-AC02-05CH112. The work at ORNL was supported by the Department of Energy, Basic Energy Sciences, Materials Sciences and Engineering Division.

References

[1] Raffius H, Mörsen E, Mosel B D, Müeller-Warmuth W, Jeitsschko W, Terbüchte L and Vomhof T 1993 *J. Phys. Chem. Solids* **54** 135
[2] Ren Z, Zhu Z, Jiang S, Xu X, Tao Q, Wang C, Feng C, Cao G and Xu Z 2008 *Phys. Rev.* B **78** 052501
[3] Xiao Y *et al* 2009 *Phys. Rev.* B **80** 174424
[4] Feng C, Ren Z, Xu S, Jiang S, Xu Z, Cao G, Nowik I and Felner I 2010 *Phys. Rev.* B **82** 094426
[5] Ryan D H, Cadogan J M, Xu S, Xu Z and Cao G 2011 *Phys. Rev.* B **83** 132403
[6] Herrero-Martín J *et al* 2009 *Phys. Rev.* B **80** 134411
[7] Uhoya W, Tsoi G, Vohra Y K, McGuire M A, Sefat A S, Sales B C, Mandrus D and Weir S T 2010 *J. Phys.: Condens. Matter* **22** 292202
[8] Sun L *et al* 2010 *Phys. Rev.* B **82** 134509
[9] Zhou B *et al* 2010 *Phys. Rev.* B **81** 155124
[10] Adhikary G, Sahadev N, Biswas D, Bindu R, Kumar N, Thamizhavel A, Dhar S K and Maiti K 2013 *J. Phys.: Condens. Matter* **25** 225701
[11] Thirupathaiah S *et al* 2011 *Phys. Rev.* B **84** 014531
[12] Marchand R and Jeitschko W 1978 *J. Solid State Chem.* **24** 351
[13] Kamihara Y, Watanabe T, Hirano M and Hosono H 2008 *J. Am. Chem. Soc.* **130** 3296
[14] Sefat A S, Jin R, McGuire M A, Sales B C, Singh D J and Mandrus D 2008 *Phys. Rev. Lett.* **101** 117004
[15] Canfield P C and Fisk Z 1992 *Phil. Mag.* B **65** 1117
[16] Neupane M *et al* 2011 *Phys. Rev.* B **83** 094522
[17] Kowalczyk S P, Edelstein N, McFeely F R, Ley L and Shirley D A 1974 *Chem. Phys. Lett.* **29** 491
[18] Shirley D A 1978 *Photoemission in Solids* (*Topics Appl. Phys.* vol 26) ed M Cardona and L Ley (Berlin: Springer) chapter 4
[19] Richard P *et al* 2010 *Phys. Rev. Lett.* **104** 137001
[20] van Heumen E *et al* 2011 *Phys. Rev. Lett.* **106** 027002
[21] Huang Y-B *et al* 2013 *Chin. Phys. Lett.* **30** 017402
[22] Richard P, Sato T, Nakayama K, Takahashi T and Ding H 2011 *Rep. Prog. Phys.* **74** 124512
[23] Nakayama K, Sato T, Terashima K, Matsui H, Takahashi T, Kubota M, Ono K, Nishizaki T, Takahashi Y and Kobayashi N 2007 *Phys. Rev.* B **75** 014513
[24] Zabolotnyy V B *et al* 2007 *Phys. Rev.* B **76** 024502
[25] Liu C, Lee Y, Palczewski A D, Yan J-Q, Kondo T, Harmon B N, McCallum R W, Lograsso T A and Kaminski A 2010 *Phys. Rev.* B **82** 075135
[26] Nishi I *et al* 2011 *Phys. Rev.* B **84** 014504
[27] Zhang P, Richard P, Qian T, Xu Y-M, Dai X and Ding H 2011 *Rev. Sci. Instrum.* **82** 043712
[28] Damascelli A 2004 *Phys. Scr.* **T109** 61
[29] Coldea A I, Andrew C M J, Analytis J G, McDonald R D, Bangura A F, Chu J-H, Fisher I R and Carrington A 2009 *Phys. Rev. Lett.* **103** 026404
[30] Xu N *et al* 2012 *Phys. Rev.* B **86** 064505

[31] Brouet V *et al* 2010 *Phys. Rev. Lett.* **105** 087001
[32] Dhaka R S *et al* 2011 *Phys. Rev. Lett.* **107** 267002
[33] Zhang Y *et al* 2011 *Phys. Rev.* B **83** 054510
[34] Reehuis M and Jeitschko W 1990 *J. Phys. Chem. Solids* **51** 961
[35] Saha S R, Butch N P, Drye T, Magill J, Ziemak S, Kirshenbaum K, Zavalij P Y, Lynn J W and Paglione J 2012 *Phys. Rev.* B **85** 024525
[36] Shi H L, Yang H X, Tian H F, Lu J B, Wang Z W, Qin Y B, Song Y J and Li J Q 2010 *J. Phys.: Condens. Matter* **22** 125702
[37] Kasahara S, Shibauchi T, Hashimoto K, Nakai Y, Ikeda H, Terashima T and Matsuda Y 2011 *Phys. Rev.* B **83** 060505
[38] Yildirim T 2009 *Phys. Rev. Lett.* **102** 037003
[39] Razzoli E *et al* 2012 *Phys. Rev. Lett.* **108** 257005